Int J Clin Exp Pathol 2017;10(10):10650-10665
www.ijcep.com /ISSN:1936-2625/IJCEP0065149

Original Article

Upregulation of HOXA13 as a potential tumorigenesis and progression promoter of LUSC based on qRT-PCR and bioinformatics

Rui Zhang[1*], Yun Deng[1*], Yu Zhang[1], Gao-Qiang Zhai[1], Rong-Quan He[2], Xiao-Hua Hu[2], Dan-Ming Wei[1], Zhen-Bo Feng[1], Gang Chen[1]

Departments of [1]Pathology, [2]Medical Oncology, First Affiliated Hospital of Guangxi Medical University, Nanning, Guangxi Zhuang Autonomous Region, China. [*]Equal contributors.

Received September 7, 2017; Accepted September 29, 2017; Epub October 1, 2017; Published October 15, 2017

Abstract: In this study, we investigated the levels of homeobox A13 (HOXA13) and the mechanisms underlying the co-expressed genes of HOXA13 in lung squamous cancer (LUSC), the signaling pathways in which the co-expressed genes of HOXA13 are involved and their functional roles in LUSC. The clinical significance of 23 paired LUSC tissues and adjacent non-tumor tissues were gathered. HOXA13 levels in LUSC were detected by quantitative real-time polymerase chain reaction (qRT-PCR). HOXA13 levels in LUSC from The Cancer Genome Atlas (TCGA) and Oncomine were analyzed. We performed receiver operator characteristic (ROC) curves of various clinicopathological features of LUSC. Co-expressed of HOXA13 were collected from MEM, cBioPortal and GEPIA. The functions and pathways of the most reliable overlapped genes were achieved from the Gene Otology (GO) and Kyoto Encyclopedia of Genes and Genomes (KEGG) databases, respectively. The protein-protein interaction (PPI) networks were mapped using STRING. HOXA13 in LUSC were markedly upregulated compared with those in the noncancerous controls as demonstrated by qRT-PCR (LUSC: 0.330±0.360; CONTROLS: 0.155±0.142; *P*=0.021). TCGA (LUSC: 6.388±2.097, CONTROLS: 1.157±0.719; *P*<0.001) and Hou's study from Oncomine (LUSC: 1.154±0.260; CONTROLS: 0.957±0.065; *P*=0.001) showed the same tendency. Meanwhile, the area under the curve (AUC) of TNM was calculated as 0.877 with *P*=0.002. Based on the HOXA13 expression data from TCGA, the ROC of the tissue types was calculated as AUC=0.971 (*P*<0.001). In addition, 506 genes were filtered as co-expression genes of HOXA13. The 3 most significant KEGG pathways were metabolic pathways (*P*=5.41E-15), the calcium signaling pathway (*P*=3.01E-11), and the cAMP signaling pathway (*P*=5.63E-11). MAPK1, GNG7, GNG12, PRKCA were selected as the hub genes. In conclusion, HOXA13 was upregulated and related to the TNM stage in LUSC. The expression of hub genes in LUSC might be deregulated by HOXA13. Moreover, the 4 co-expressed hub genes of HOXA13 might be crucial biomarkers for the diagnosis and prognosis of LUSC, as well as the development of novel therapeutic targets against LUSC.

Keywords: HOXA13, lung squamous cancer, potential mechanisms, bioinformatics

Introduction

Lung cancer is one of the most frequent cancers occurring in men and women in 2017, as well as a worldwide leading cause of cancer deaths [1]. As a life-threatening disease, it is categorized into two different major groups: non-small cell lung cancer (NSCLC) and small cell lung cancer (SCLC). At least 80%-85% of all lung tumors belong to NSCLC. LUSC and lung adenocarcinomas (LUAD) are the most common histological subtypes of NSCLC [2-5]. In addition, due to the high prevalence of smoking, about 30% of lung cancer patients were diagnosed as the squamous histopathological subtype [6]. The survival rate of advanced LUSC patients remains poor, only less than 5% of patients surviving 5 years after chemotherapeutic regimens [7]. Although tobacco smoke causes lung cancer was well established, not all lung cancer patients respond to it. Dysregulated genetic factors are speculated to play an important role in lung cancer susceptibility.

The homeobox genes were discovered in Drosophila firstly, where their mutations could cause

Table 1. The clinical significance of 23 LUSC patients

Clinical significance		N
Clinicopathological types	LUSC	23
	Adjacent non-cancerous tissues	23
Tumor size	≤3 cm	7
	>3 cm	16
TNM stage	I-II	10
	III-IV	13
Gender	Male	18
	Female	5
Age	<60 years	15
	≥60 years	8
Smoking	Yes	11
	No	12
Vascular invasion	Yes	3
	No	20
Grading	I	0
	II	16
	III	7

Note: TNM, tumor-node-metastasis.

the malformations of body parts in inappropriate contexts [8, 9]. Both class I (HOX) and class II (non-HOX) are generally belong to homeobox genes. A total of 39 HOX genes have been identified in humans and are clustered into 4 groups named A, B, C and D, respectively. In addition, each member of HOX genes in a cluster is named from 1 to 13 [10, 11]. Different clusters of homeobox genes play essential roles in embryonic morphogenesis, including organ systems, skeletal, limb and craniofacial region. In adults, homeobox genes also regulate tissue regeneration and play fundamental roles for the control of the self-renewal and differentiation of hematopoietic progenitors [8, 12, 13]. A lot of studies have reported that abnormal levels of HOX genes in certain organs could either suppress tumors or promote tumors, including the prostate [14], ovary [15], breast [16], kidney [17], and lung [18, 19]. Altered expression of HOXA genes were reported in breast and ovarian cancers. In colon cancers, both HOXB and HOXD genes were dysregulated. Moreover, aberrantly expressed HOXC genes were indicated in prostate and lung cancers [20]. Based on the gene amplification, loss of heterozygosity, histone deacetylation and CpG island promoter hypermethylation, dysregulated HOX genes would facilitate the development and progression of cancers consequently [21]. As a member of the homeobox genes, HOXA13 has an oncogene-like character in multiple cancers. HOXA13 can enhance gastric cancer cell invasion and the epithelial-to-mesenchymal transition (EMT) via the TGF-β signaling pathway. Upregulation of HOXA13 is related to a poorer prognosis of gastric cancer patients [22, 23]. In prostate cancer, both cell growth and cell cycle were closely associated with downregulated HOXA13. Lower HOXA13 exerts a role of tumor-suppressor and provides a potential therapeutic approach against this malignancy [24]. In part, HOXA13 promotes progression of glioma and would be helpful to diagnose glioblastoma. HOXA13 was also revealed to be an independent prognostic factor especially in high-grade glioma [25].

However, the probable mechanisms and pathways of HOXA13 in lung cancer have rarely been reported. Sang Y et al. found that HOTTIP was a transcriptional modulator of HOXA13 and partly regulated HOXA13 to promote cell proliferation, migration, and inhibit apoptosis of lung cancer cell [26]. Kang JU et al. demonstrated that rearranged 7p arm of HOXA13 (7p15.2) may be a valuable potential target and a therapeutic target for LUAD [27]. In this study, we aimed to investigate the potential roles of HOXA13 in LUSC. The clinical significance of HOXA13 in LUSC was gathered from qRT-PCR results and the TCGA and Oncomine databases. Meanwhile, the potential mechanisms and pathways of the co-expressed genes of HOXA13 in LUSC were predicted. Moreover, the correlated functions between HOXA13 and its several pivotal co-expressed genes in LUSC were studied based on the aforementioned information.

Methods and materials

Clinicopathological significance

Sample collection: 23 paired LUSC and adjacent non-cancerous lung tissues were obtained from patients who performed surgery at The First Affiliated Hospital of Guangxi Medical University between January 2012 and February 2014 and were histopathologically diagnosed with LUSC. The clinicopathological information of the patients is shown in **Table 1**. The study

Table 2. Correlations between clinical significance and expression of HOXA13 in LUSC

Clinical significance		N	LUSC expression condition ($2^{-\Delta X0}$)			
			Mean	SD	t (or F)	*P* value
Clinicopathological types	LUSC	23	0.330	0.360	2.480	0.021
	Adjacent non-cancerous tissues	23	0.155	0.142		
Tumor size	≤3 cm	7	0.414	0.484	0.732	0.472
	>3 cm	16	0.294	0.303		
TNM stage	I-II	10	0.112	0.072	-3.385	0.005
	III-IV	13	0.499	0.404		
Gender	Male	18	0.349	0.394	0.461	0.650
	Female	5	0.264	0.212		
Age	<60 years	15	0.340	0.368	0.170	0.867
	≥60 years	8	0.313	0.369		
Smoking	Yes	11	0.472	0.461	-1.846	0.089
	No	12	0.201	0.166		
Vascular invasion	Yes	3	0.466	0.176	-0.693	0.496
	No	20	0.310	0.379		
Grading	I	0	-	-	0.788	0.385
	II	16	0.375	0.412		
	III	7	0.229	0.183		

Note: t, Student's t-test; F, one-way ANOVA; SD, standard deviation; TNM, tumor-node-metastasis.

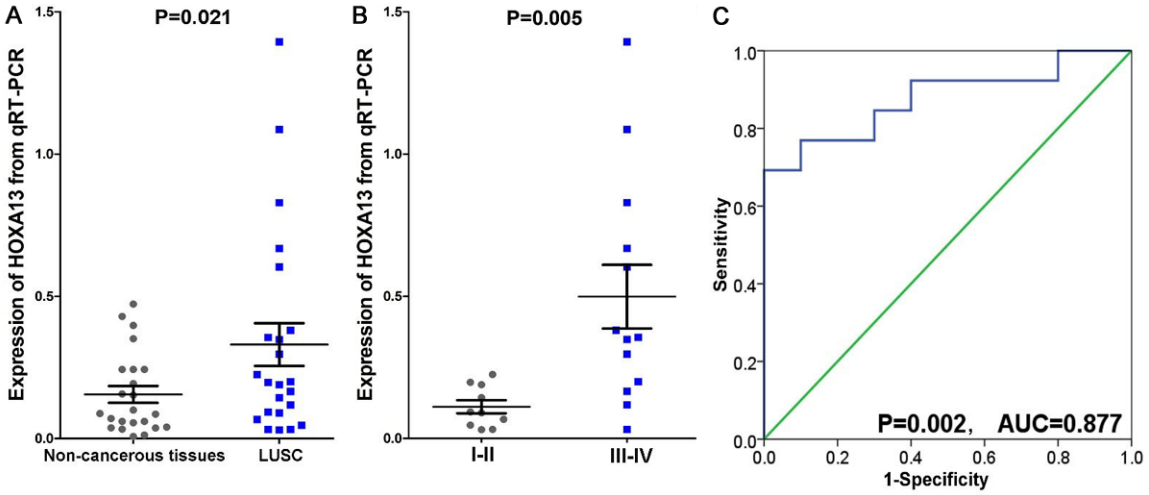

Figure 1. qRT-PCR results of HOXA13 levels in LUSC. A. Expression of HOXA13 in LUSC and non-cancerous tissues from qRT-PCR; B. HOXA13 levels in different TNM stages from qRT-PCR; C. ROC of HOXA13 in different TNM stages.

was undertaken with the understanding and written consent of each patient.

RNA extraction and qRT-PCR assay: Total RNA was extracted from FFPE tissues using the RNeasy reagent (QIAGEN, Shanghai, China) according to the manufacturer's instructions. We used the ND-2000 NanoDrop system (Thermo-Scientific, USA) to detect the concentration and purity of RNA, and the A260/280 ratio was 1.8-2.0. According to the manufacturer's instructions, total RNA was reverse transcribed in a final volume of 10 μl using a reverse transcription kit (ABI, Life Technologies, USA). Fluorochrome SYBR Green I Master was used to establish a 20-μL real-time fluorescence PCR system. The PCR procedure was described as follows: initial denaturation at 95°C for 10 min,

Table 3. Clinicopathological features of HOXA13 in LUSC based on TCGA

Clinicopathological features		N	HOXA13 expression		
			Mean ± SD	t (or F)	*P* value
Tissues	Cancer	470	6.387±2.097	-19.232	<0.001
	Non-cancerous	8	1.157±0.719		
Race	White	331	5.465±2.051	F=3.892	0.021
	Asian	9	4.264±2.662		
	Black	28	6.304±1.585		
AGE	≥60 years	198	6.341±2.105	-0.345	0.730
	<60 years	40	6.470±2.377		
Gender	Male	349	6.471±2.081	1.475	0.141
	Female	121	6.145±2.133		
Status	Dead	201	6.272±2.154	-1.030	0.304
	Alive	269	6.473±2.054		
Neoplasm Cancer Status	With tumor	105	6.247±2.268	-0.678	0.500
	Tumor free	299	6.410±2.0725		
Stage	I-II	382	6.492±2.040	1.798	0.073
	III-IV	84	6.043±2.211		
M	M0	390	5.549±2.069	F=0.224	0.800
	M1	4	6.041±2.528		
	MX	73	5.431±1.974		
T	T1-T2	385	6.432±2.015	0.881	0.380
	T3-T4	85	6.182±2.439		
N	N0-N1	424	5.525±2.050	F=2.566	0.078
	N2-N3	45	5.780±1.974		
	NX	4	3.369±2.596		
Recurrence	Distant metastasis	36	5.524±2.346	F=0.565	0.571
	New primary tumor	12	5.457±2.031		
	Locoregional recurrence	30	4.959±2.135		

Note: t, Student's t-test; F, one-way ANOVA; SD, standard deviation; T, tumor; N, lymph node; M, metastasis.

denaturation at 95°C for 10 s; refolding for 5 s at annealing temperature 60°C; extension at 72°C for 5 s (a total of 40 cycles). The specific primers used were as follows: HOXA13 forward primer: 5'-GAACGGCCAAATGTACTGCC-3', reverse primer: 5'-CGCCTCCGTTTGTCCTTAGT-3'. GAPDH (internal control) forward primer: 5'-TGCACCACCAACTGCTTA-3', reverse primer: 5'-GGATGCAGGGATGATGTTC-3'. The expression difference was calculated using the $2^{-\Delta X\theta}$ method [28, 29].

TCGA data downloading: From TCGA (http://cancergenome.nih.gov), the raw count of mRNAs (level 3) and clinical parameters of LUSC patients were downloaded. The HOXA13 levels in LUSC and AUC values of ROC were calculated based on the TCGA data. AUC values of ROC were calculated using GraphPad Prism 5. Meanwhile, the overall survival (OS) and disease free survival (DFS) of LUSC patients were evaluated by SPSS 22.0.

Oncomine data mining: To further verify the level of HOXA13 in LUSC, we amplified multiple Oncomine expression analyses for HOXA13 in LUSC datasets with expression levels (https://www.oncomine.org). HOXA13 levels in different cases were shown in scatter diagrams using GraphPad Prism 5.0.

Bioinformatics analysis

Genes extraction and KEGG pathway prediction: Genes expressed similarly to HOXA13 were extracted from 3 different datasets, including MEM (http://biit.cs.ut.ee/mem), cBioPortal (http://www.cbioportal.org), and GEPIA (http://gepia.cancer-pku.cn). The overlapped

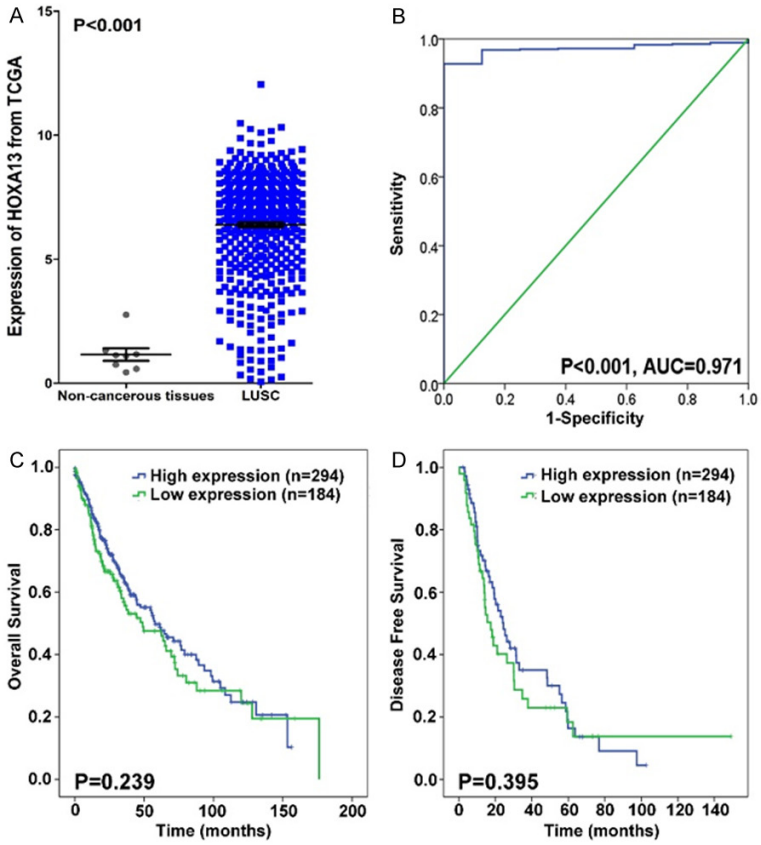

Figure 2. Data of HOXA13 expression levels and KM curves from TCGA. A. Expression of HOXA13 from TCGA database; B. HOXA13's ROC curve in TCGA; C. Kaplan-Meier plots of overall survival (months); D. Kaplan-Meier plots of disease free survival (months).

genes in any 2 or 3 datasets were chosen. For a higher quality of results, the intersected genes were used to analyze KEGG pathways by DAVID (https://david.ncifcrf.gov) [30, 31]. The genes involved in various significant pathways were selected as co-expression genes of HOXA13 for further analysis.

Enrichment analysis and PPI networks: Based on the co-expression genes of HOXA13, GO term enrichment analysis was performed using Cytoscape 3.5.1. The PPI networks were mapped by STRING (http://www.string-db.org). In addition, the genes acting on others over 50 times would be selected as our hub genes in the current study. The correlations between hub genes and HOXA13 were evaluated by GraphPad Prism 5.0.

Statistical analysis

All statistical analyses were performed using SPSS 22.0 statistics software (SPSS, Chicago, USA). The clinical follow-up data of HOXA13 levels in LUSC provided by PCR and TCGA were listed as the means ± standard deviation (SD). For the parametric data of clinical features, the means of 2 continuous variables were compared using independent samples Student's t-test. The means of 2 paired variables were calculated by paired Student's t-test. Comparison of more than two different groups was performed by one-way ANOVA. The OS and DFS rates were plotted utilizing the Kaplan-Meier method. The correlations between HOXA13 and hub genes were calculated by Pearson Correlation. A *P*-value <0.05 indicated statistical significance.

Results

Clinical significance

PCR data: The results of qRT-PCR are shown in **Table 2**. HOXA13 was expressed at a significantly higher level in LUSC tissues (0.330±0.360) than in non-cancerous tissues (0.155±0.142) (*P*=0.021). In TNM I-II (0.112±0.072), the levels of HOXA13 were significantly lower than those in TNM III-IV (0.499±0.404) (*P*=0.005). Meanwhile, the AUC of TNM was calculated as 0.877 with *P*=0.002 (**Figure 1**). HOXA13 expression conditions for other clinical features showed no significant outcomes.

TCGA data: In the TCGA datasets, the HOXA13 levels in LUSC tissues and non-cancerous controls were 6.387±2.097 and 1.157±0.719, respectively, with a *P* value <0.001. Among the three races, HOXA13 was expressed the highest in Black individuals (6.304±1.585), followed by White individuals (5.465±2.051) and Asian individuals (4.264±2.662) (*P*=0.021) (**Table 3**). The ROC of the tissue types was calculated as AUC=0.971 (*P*<0.001). Unfortunately, no significance was found in both survival rate of OS and DFS (**Figure 2**).

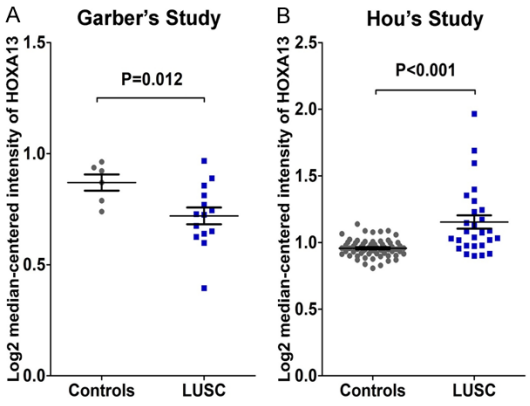

Figure 3. Two related studies of HOXA13 levels in LUSC. A. HOXA13 in LUSC in Garber's study; B. Levels of HOXA13 in LUSC from Hou's study.

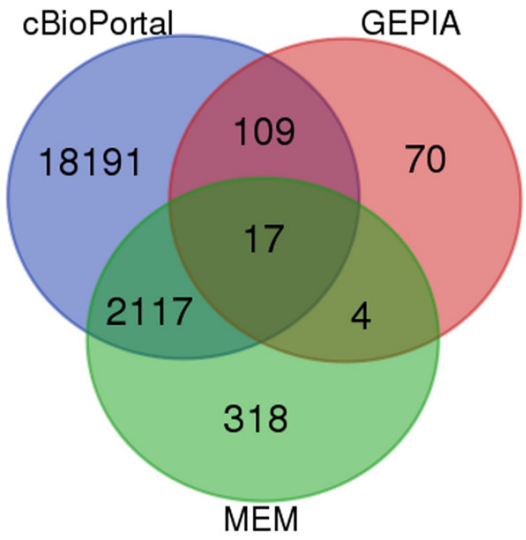

Figure 4. Intersected genes achieved from Venn. Each circle filled with different color represents a different platform. The numbers are the counts of genes.

Oncomine data: Two datasets related to HOXA13 and LUSC were extracted. In Hou's study [32], 65 controls and 27 LUSC cases were found. Meanwhile, 6 controls and 14 LUSC samples were obtained from Garber's study [33]. HOXA13 levels increased in LUSC tissues in Hou's study (P<0.001). By contrast, Garber reported that HOXA13 levels were decreased in LUSC tissues compared with those in the controls (P=0.012) (**Figure 3**).

Bioinformatics analysis

Extraction of similarly expressed genes of HOXA13: In MEM, 4 different probesets of HOXA13 in the human genome were filtered. The output limitation of the genes was set as 1,500 per probesets. Finally, 2,456 different genes were obtained. Meanwhile, 20,434 genes, whose expressions were similar to that of HOXA13 in LUSC, were obtained from cBioPortal. From GEPIA, the 200 most similarly expressed genes associated with HOXA13 in LUSC were selected. A total of 2,565 intersected genes in 2 or 3 datasets were extracted as shown in Veen diagram (**Figure 4**). After removing the repetitive genes, 2,247 genes were saved for further analysis.

KEGG pathway annotation and co-expression gene collection: Based on 2,247 selected genes, KEGG pathway annotation was performed. As shown in **Table 4**, the first three significant pathways were calcium signaling pathway (P=1.01E-05), cAMP signaling pathway (P=2.36E-05), and proteoglycans in cancer (P=6.73E-05). For a higher quality of results, the genes involved in all significant KEGG pathways were pooled together. Ultimately, 506 more reliable co-expression genes of HOXA13 in LUSC were selected, and KEGG pathway annotation was re-performed (**Table 5**). The first three pathways were metabolic pathways (P=5.41E-15), the calcium signaling pathway (P=3.01E-11), and the cAMP signaling pathway (P=5.63E-11).

Enrichment analysis: Five hundred six co-expression genes of HOXA13 were annotated in GO. There were three categories of GO, including biological process (BP), molecular function (MF), and cellular component (CC). The top 5 most significantly enriched pathways of each category are shown in **Table 6**. In the BP category, the most significant pathway was axon guidance (6.63E-09). Additionally, in the MF and CC categories, the most significantly enriched pathways were ATP binding (8.62E-08) and cytosol (1.08E-17), respectively.

PPI network: The PPI network contained 485 items (**Figure 5**). The top 10 interacting gene pairs with the highest combined score are listed in **Table 7**. Moreover, MAPK1, GNG7, GNG12, PRKCA were selected as hub genes in this study. In addition to MAPK1, the remaining three hub genes were all significantly decreased in LUSC tissues in **Figure 6** (P<0.001). In addition, there was no significant correlations between the levels of hub genes and HOXA13 in LUSC (**Figure 7**).

Table 4. Top 10 significant KEGG pathways of 2,247 co-expressed genes of HOXA13

Term	Count	*P* Value	Genes
Calcium signaling pathway	41	1.01E-05	ADCY1, GNA11, CAMK2G, DRD5, OXTR, BDKRB2, ITPKA, ATP2B1, PRKACG, ATP2B2 etc.
cAMP signaling pathway	43	2.36E-05	PPARA, ATP1B1, ADCY1, ATP1B3, GNAI1, CAMK2G, DRD5, ADCY6, OXTR, GRIN3B etc.
Proteoglycans in cancer	42	6.73E-05	WNT5B, LUM, PPP1R12B, CAMK2G, PPP1R12C, TLR4, PDCD4, ITGB1, HOXD10, PRKACG etc.
Peroxisome	23	7.31E-05	ACOX2, NUDT19, EHHADH, AMACR, CRAT, PEX11G, PEX11A, PEX11B, FAR2, MLYCD etc.
Glutamatergic synapse	28	9.83E-05	SLC38A3, ADCY1, GNAI1, ADCY6, GNG13, GRIK5, GRIN3B, GNG12, KCNJ3, PRKACG etc.
Axon guidance	30	1.11E-04	NRP1, GNAI1, EFNA2, EFNA3, L1CAM, EPHB3, EPHB4, ITGB1, SEMA5A, SEMA7A etc.
Cholinergic synapse	27	1.60E-04	ADCY1, GNAI1, CAMK2G, GNA11, ADCY6, GNG13, GNG12, KCNJ3, PRKACG, KCNQ4 etc.
Endocrine and other factor-regulated calcium reabsorption	15	2.46E-04	PRKCA, ATP1B1, CLTB, ATP1B3, KLK2, ADCY6, PRKCG, BDKRB2, KLK1, PRKACG, VDR etc.
Insulin secretion	22	3.09E-04	PRKCA, TRPM4, ATP1B1, ADCY1, ATP1B3, CAMK2G, GNA11, ADCY6, FFAR1, PRKCG etc.
Pancreatic secretion	23	4.33E-04	PRKCA, ATP1B1, PNLIPRP1, ADCY1, ATP1B3, SLC12A2, ADCY6, PRKCG, ITPR3, ATP2B1 etc.

Table 5. Top 10 significant KEGG pathways annotations of 506 higher qualified co-expressing genes of HOXA13

Term	Count	*P* Value	Genes
Metabolic pathways	156	5.41E-15	ALAD, SGMS2, NT5C3A, EHHADH, PTGS1, PPCS, PI4K2B, ACSS2, NMRK1, ITPKA etc.
Calcium signaling pathway	41	3.01E-11	ADCY1, GNA11, CAMK2G, DRD5, OXTR, BDKRB2, ITPKA, ATP2B1, PRKACG, ATP2B2 etc.
cAMP signaling pathway	43	5.63E-11	PPARA, ATP1B1, ADCY1, ATP1B3, GNAI1, CAMK2G, DRD5, ADCY6, OXTR, GRIN3B etc.
Pathways in cancer	64	2.92E-10	FGF6, ADCY1, PPARD, GNA11, ADCY6, PPARG, LPAR1, PTEN, PRKACG, PLCB3 etc.
Proteoglycans in cancer	42	2.95E-10	WNT5B, LUM, PPP1R12B, CAMK2G, PPP1R12C, TLR4, PDCD4, ITGB1, HOXD10, PRKACG etc.
Endocytosis	46	9.05E-09	CLTB, CHMP3, TSG101, CHMP4B, CAPZA2, STAM2, KIAA0196, ASAP2, PIP5K1B, ASAP1 etc.
Axon guidance	30	1.02E-08	NRP1, GNAI1, EFNA2, EFNA3, L1CAM, EPHB3, ITGB1, EPHB4, SEMA5A, SEMA7A etc.
Glutamatergic synapse	28	1.45E-08	SLC38A3, ADCY1, GNAI1, ADCY6, GNG13, GRIK5, GRIN3B, GNG12, KCNJ3, PRKACG etc.
Focal adhesion	39	2.93E-08	TLN2, PPP1R12B, PPP1R12C, ARHGAP35, MYL10, PTEN, ITGB1, LAMB3, ARHGAP5, ITGB8 etc.
Neuroactive ligand-receptor interaction	47	2.98E-08	TSPO, THRA, THRB, DRD5, GRIK5, OXTR, GRIN3B, BDKRB2, LPAR1, VIPR1 etc.

Table 6. Top 5 most significant enriched pathways of BP, MF and CC categories

Category	Term	Count	*P* Value	Genes
GOTERM_BP_DIRECT	Axon guidance	22	6.63E-09	NRP1, KIF5B, EFNA2, EFNB2, EFNA3, NTN4, ARHGAP35, L1CAM, EPHB3, SLIT2 etc.
GOTERM_BP_DIRECT	Positive regulation of cell migration	23	1.87E-08	PRKCA, EGFR, BMP4, WNT5B, SMAD3, HGF, SEMA5A, MAPK1, SEMA6B, SEMA6C etc.
GOTERM_BP_DIRECT	Semaphorin-plexin signaling pathway	11	1.91E-08	SEMA5A, SEMA6B, NRP1, SEMA6C, SEMA4G, SEMA3F, SEMA7A, RAC1, MET, SEMA3C, SEMA3B
GOTERM_BP_DIRECT	Neural crest cell migration	12	4.45E-08	SEMA5A, SEMA6B, SEMA6C, SEMA4G, SEMA3F, SEMA7A, KITLG, SEMA3C, SEMA3B, ISL1, HTR2B, ACVR1
GOTERM_BP_DIRECT	Response to drug	29	7.15E-08	ALAD, TSPO, ADCY1, ASS1, PPARG, OXTR, PDX1, PTEN, MTHFR, GATA4 etc.
GOTERM_MF_DIRECT	Atp binding	80	8.62E-08	ATP1B1, ADCY1, ADCY6, PIP5K1B, HLCS, PI4K2B, ACSS2, ITPKA, NMRK1, INSRR etc.
GOTERM_MF_DIRECT	Semaphorin receptor binding	8	2.61E-06	SEMA5A, SEMA6B, SEMA6C, SEMA4G, SEMA3F, SEMA7A, SEMA3C, SEMA3B
GOTERM_MF_DIRECT	Chemorepellent activity	8	8.57E-06	SEMA5A, SEMA6B, SEMA6C, SEMA4G, SEMA3F, SEMA7A, SEMA3C, SEMA3B
GOTERM_MF_DIRECT	Calmodulin binding	19	9.50E-06	TRPM4, EGFR, SLC8A1, ADCY1, CAMK2G, GRIN1, IQGAP3, ITPKA, ATP2B1, ATP2B2 etc.
GOTERM_MF_DIRECT	Drug binding	12	1.08E-05	P2RX4, PPARA, ATP1B1, PPARD, PPARG, CHRNB2, PDE4D, PPP3CA, RARB, HTR2B, AOC1, CHRNA2
GOTERM_CC_DIRECT	Cytosol	167	1.08E-17	ALAD, CHMP3, THRA, NT5C3A, CHMP4B, EHHADH, CAPZA2, PPP2R5C, IQGAP3, PPCS etc.
GOTERM_CC_DIRECT	Plasma membrane	187	3.88E-15	ATP1B1, ADCY1, CHMP3, ATP1B3, SGMS2, EFNA2, GNA11, EFNA3, GDF5, ADCY6 etc.
GOTERM_CC_DIRECT	Extracellular exosome	133	1.79E-11	ATP1B1, TSPO, ALAD, ADCY1, CHMP3, ATP1B3, THRB, CHMP4B, CAPZA2, GNA11 etc.
GOTERM_CC_DIRECT	Peroxisome	20	3.48E-11	ACOX2, EHHADH, AMACR, CRAT, PEX11G, PEX11A, PEX11B, FAR2, MLYCD, GSTK1 etc.
GOTERM_CC_DIRECT	Peroxisomal matrix	13	2.02E-09	ACOX2, FAR2, NUDT19, MLYCD, EHHADH, AMACR, IDH1, ABCD3, CAT, CRAT, SCP2, CROT, ACAA1

Note: BP, biological process; MF, molecular function; CC, cellular component.

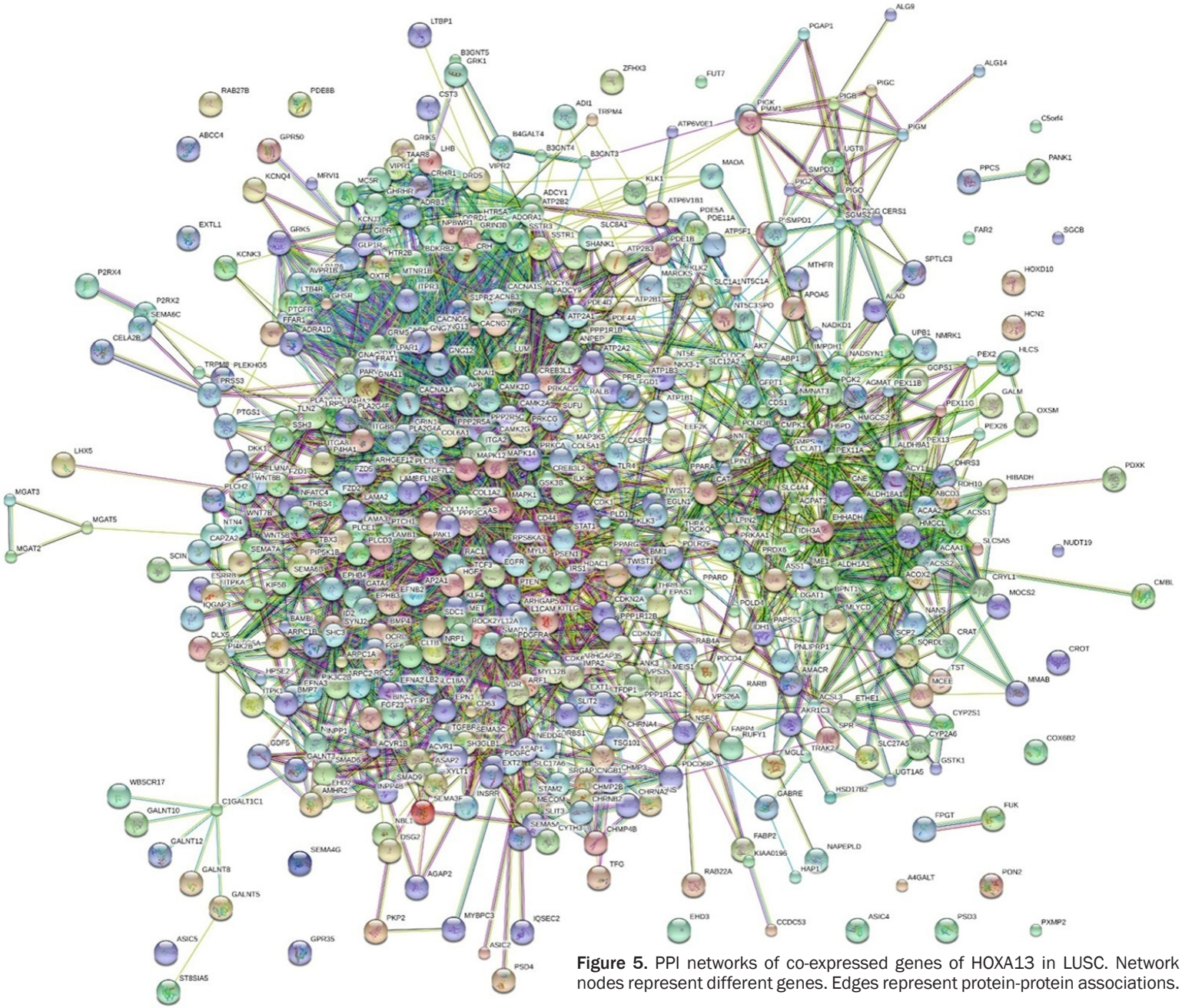

Figure 5. PPI networks of co-expressed genes of HOXA13 in LUSC. Network nodes represent different genes. Edges represent protein-protein associations.

Table 7. Top 10 interacted genes pairs with the highest combined score

Node 1	Node 2	Neighborhood_ on_chromosome	Gene_ fusion	Phylogenetic_ cooccurrence	Homology	Coexpression	Experimentally_determined_ interaction	Database_ annotated	Automated_ textmining	Combined_ score
VPS35	VPS26A	0	0	0	0	0.198	0.996	0.9	0.961	0.999
EPHB4	EFNB2	0	0	0	0	0.405	0.651	0.9	0.961	0.999
ACAA1	EHHADH	0.505	0.117	0	0	0.678	0.94	0.951	0.832	0.999
CHMP3	CHMP4B	0	0	0	0	0.225	0.977	0.9	0.587	0.999
PARVA	ILK	0	0	0	0	0.12	0.993	0.9	0.941	0.999
CAMK2A	CAMK2D	0	0	0.527	0.987	0	0.993	0.9	0.389	0.999
ARPC5	ARPC2	0	0	0	0	0.222	0.984	0.9	0.905	0.999
PSEN1	APP	0	0	0	0	0.048	0.406	0.9	0.987	0.999
GMPS	IMPDH1	0.505	0	0.352	0	0.952	0.928	0.951	0.689	0.999
ARPC2	ARPC1B	0	0	0	0	0.149	0.968	0.9	0.878	0.999

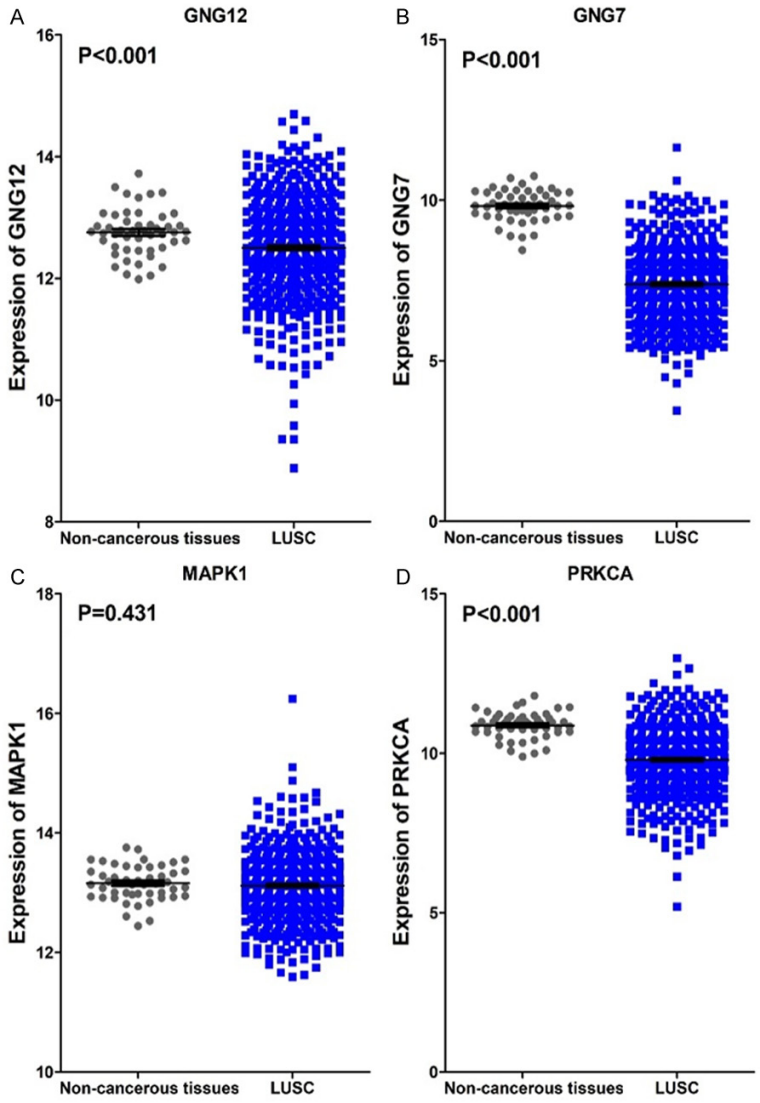

Figure 6. The 4 hub genes expression levels in LUSC. A. GNG12 levels in tissues of LUSC and non-tumor tissues; B. The gene GNG7 expressing conditions in LUSC and non-cancerous tissues; C. Comparison of MAPK1 levels in LUSC and controls; D. Expression of PRKCA in LUSC and normal tissues.

Discussion

HOX family members were known as a class of remarkable development-associated genes, aberrant expression of HOX genes have been discovered in many studies related to various solid tumors. In the present study, an increased level of HOXA13 in LUSC tissues was verified by qRT-PCR. The same expression trends were found in TCGA and Hou's study [32] from Oncomine. However, Garber's study [33] from Oncomine showed an inverse trend in the HOXA13 level such that it was expressed higher in controls than in LUSC tissues. Abate-Shen et al. proposed three mechanisms that drive the deregulation of aberrant HOX genes expression, including temporospatial deregulation, gene dominance and epigenetic deregulation. The first two mechanisms were demonstrated to be generally occurred in tumorigenesis which caused by HOX genes. Inversely, epigenetic deregulation could be found evidently in tissues when HOX genes function as tumor suppressor [34]. High HOXA13 in LUSC might be closely associated with temporospatial deregulation and gene dominance. Moreover, based on the results from qRT-PCR, HOXA13 was significantly higher in TNM III-IV than in TNM I-II. Our findings suggest that HOXA13 is likely involved in the tumorigenesis and progression of LUSC.

Among all the pathways predicted by the co-expression genes of HOXA13, "metabolic pathways" was the most significant. Metabolism is involved directly or indirectly in essentially all activities of a cell. In human lung cancer cell, metabolic reprograming of tumor cell directly connects to tumor evasion caused by the immune response [35]. It is concluded that most NSCLC cases are characterized by an orchestrated activation of glucose absorption and metabolism toward anaerobic pathways [36]. Moreover, phosphoglycerate dehydrogenase describes a unique metabolic program which is activated in a lung adenocarcinoma subset. This metabolic program could confer growth of malignancy and survival and may have therapeutic implications [37]. As a specific metabolism feature, upregulated GLUT1 and glycolytic metabolism could accelerate targeted treatment of LUSC. It also has been shown to be related to define histological subtypes of metabolic dependencies within NSCLC [5]. Broadly, vast factors were

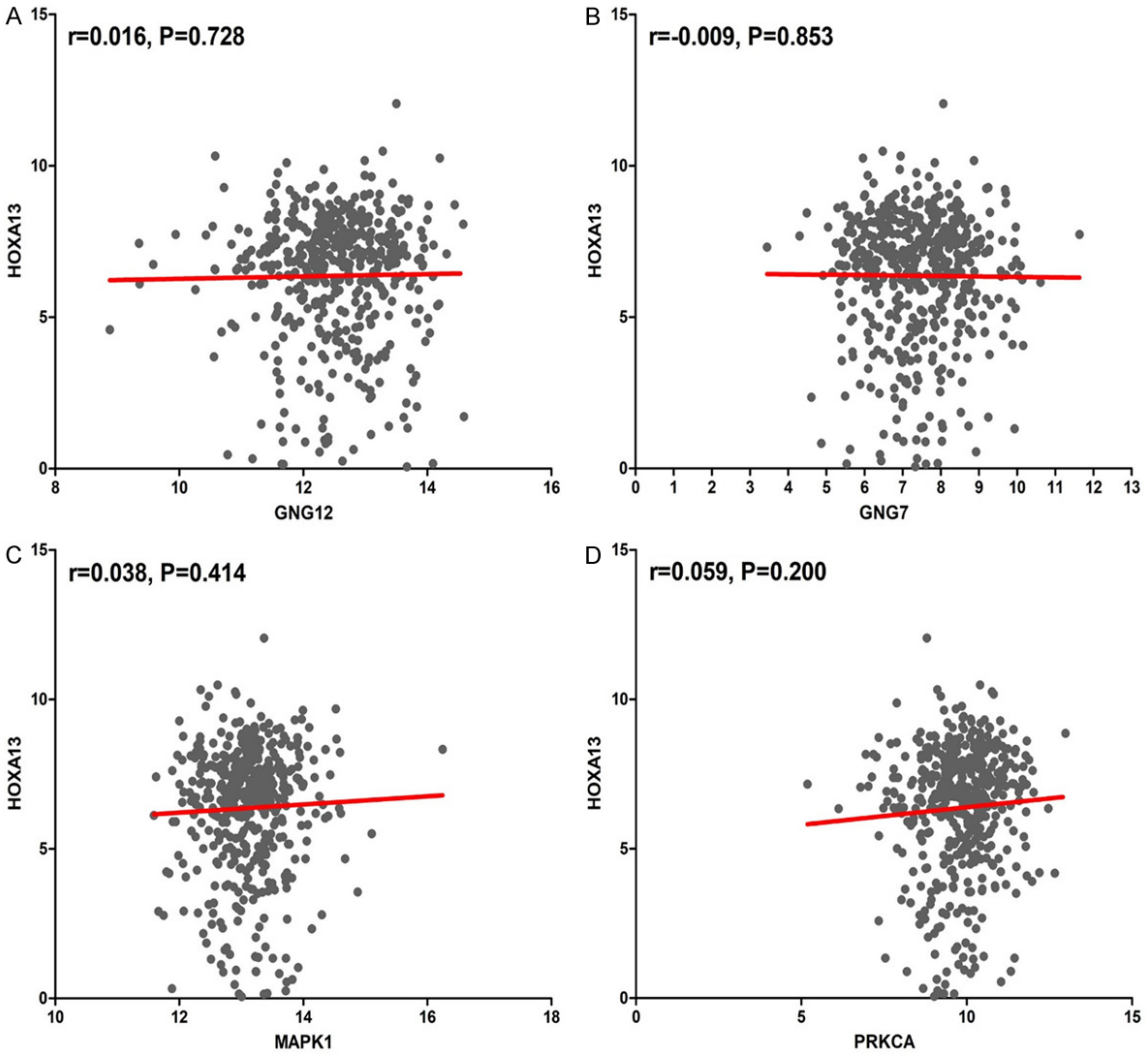

Figure 7. Correlations of 4 hub genes and HOXA13 in LUSC. A. Correlations between HOXA13 and GNG12; B. Correlations between HOXA13 and GNG7; C. Correlations between HOXA13 and MAPK1; D. Correlations between HOXA13 and PRCKA.

reported to be associated with metabolism in NSCLC. However, no clear mechanisms of metabolism have been described thus far in LUSC. Therefore, more comprehensive evidence of metabolic factors in carcinogenesis and development of LUSC should be validated. In addition, previous studies have reported relevant functions of the calcium signaling pathway. In the trisphosphate/calcium signaling pathway, generated Ca^{2+} could directly control metabolism, proliferation, smooth muscle contraction and so on [38]. Radioresistance of NSCLC cells could also be promoted by intracellular Ca^{2+} through the phosphorylation of the Akt signaling pathway [39]. Furthermore, tumor-related calcium signal transducer 2 (trop2) was identified to be correlated with tumor proliferation and invasion of NSCLC. Trop2 promoted the neovascularization of NSCLC via the activation of the ERK1/2 signaling pathway [40]. In the future, protein A2 combined with S100 calciummay serve as a dependable biomarker for the diagnosis and prognosis of NSCLC [41]. We deduced that Ca^{2+} might regulate multiple clinicopathological features of LUSC, such as tumorsize and vascular invasion conditions. Additionally, proteins and pathways related to Ca^{2+} might provide a novel strategy for LUSC treatment. As a second messenger that mobilize signaling pathways, 3',5'-Cyclic adenosine monophosphate (cAMP) regulates various cellular functions, such as metabolism, cell prolif-

eration, gene transcription, and cell migration [42]. The cAMP signaling system could induce the apoptosis of lung cancer cells [43]. cAMP signaling also modulates human lung cancer cell death induced by anticancer drugs [44]. Thus, deeper insights into the mechanisms of cAMP signaling pathways in NSCLC would be beneficial to LUSC treatment.

MAPK1, GNG7, GNG12, and PRKCA are the primary genes closely related to HOXA13 in LUSC. These 4 hub genes were all involved in the significant annotation of 'pathways in cancers'. Both guanine nucleotide binding protein 7 (GNG7) and 12 (GNG12) are members of the large G protein gamma family. Previous studies have discovered that GNG7 might block proliferation of cells in multicellular organisms [45]. Downregulated GNG7 was found in many cancers, such as pancreatic cancer [46], esophageal cancer [47], and gastrointestinal tract cancer [45]. These results were consistent with a lower level of GNG7 in LUSC in this study. Therefore, we speculated that GNG7 might play a novel therapeutic role in LUSC by inhibiting the growth of cancer cells. Moreover, in living cells, protein kinase C phosphorylates GNG12 when receptors and G proteins are activated [48]. The regulator of G protein signaling 20 (RGS20) and G protein-coupled receptor 56 (GPR56) could both enhance cell invasion [49, 50]. Downregulated GNG12 might be an important oncogene in LUSC due to the deregulation and functions of various G proteins. In addition, MAPK1 might be responsible for the development of smoking-induced lung cancer [51]. In LUSC cell lines which derived from the tongue, larynx and lung, MAPK1 was indicated as a crucial downstream signal transducer [52]. Additionally, it would help to predict the outcomes of patients with LUSC and improve the treatment strategies [53]. Furthermore, the amoeboid morphology of tumor cells could be maintained by PRKCA. Serum-activated PRKCA is a reliable biomarker applicable to lung cancer diagnosis [54, 55]. Meanwhile, PRKCA is identified as an effective therapeutic target for antimetastasis and lung cancer treatment due to its important role in both mesenchymal and amoeboid invasiveness [56, 57]. In LUSC, GNG7, GNG12 and PRKCA showed an inverse trend in LUSC compared with HOXA13. They were significantly decreased in LUSC tissues. Therefore, we hypothesized that HOXA13 might hinder their transcription via binding to their promoters or key signaling pathways. However, no significant direct evidence between HOXA13 and the hub genes in LUSC have been reported. The relationship between HOXA13 and the hub genes is still needed to be validated by more experiments in the future.

In conclusion, our results showed that HOXA13 is upregulated and associated with the TNM stage in LUSC. The pathway annotations are helpful to elucidate the mechanisms of LUSC. HOXA13 might hinder the transcription of hub genes in LUSC. Moreover, the 4 crucial co-expression hub genes of HOXA13 might be potential biomarkers for the diagnosis and prognosis of LUSC, as well as the development of novel therapeutic targets against LUSC.

Acknowledgements

The present study was supported by the Fund of National Natural Science Foundation of China (NSFC81560386), the Natural Science Foundation of Guangxi, China (2016GXNSFBA380039) and the Promoting Project of Basic Capacity for University Young and Middle-aged Teachers in Guangxi (KY2016LX031). We also wish to thank the public databases, such as the Gene Expression Omnibus functional genomics data repository, The Cancer Genome Atlas dataset and so on.

Disclosure of conflict of interest

None.

Address correspondence to: Drs. Zhen-Bo Feng and Dan-Ming Wei, Department of Pathology, First Affiliated Hospital of Guangxi Medical University, 6 Shuangyong Road, Nanning 530021, Guangxi Zhuang Autonomous Region, China. Tel: +86 771 5352194; Fax: +86 771 5352194; E-mail: Fengzhenbo_GXMU@163.com (ZBF); danmingwei08@163.com (DMW)

References

[1] Siegel RL, Miller KD and Jemal A. Cancer statistics, 2017. CA Cancer J Clin 2017; 67: 7-30.

[2] Tiran V, Lindenmann J, Brcic L, Heitzer E, Stanzer S, Tabrizi-Wizsy NG, Stacher E, Stoeger H, Popper HH, Balic M and Dandachi N. Primary patient-derived lung adenocarcinoma cell culture challenges the association of cancer stem

cells with epithelial-to-mesenchymal transition. Sci Rep 2017; 7: 10040.
[3] Jiang L, Zhu W, Streicher K, Morehouse C, Brohawn P, Ge X, Dong Z, Yin X, Zhu G, Gu Y, Ranade K, Higgs BW, Yao Y and Huang J. Increased IR-A/IR-B ratio in non-small cell lung cancers associates with lower epithelial-mesenchymal transition signature and longer survival in squamous cell lung carcinoma. BMC Cancer 2014; 14: 131.
[4] Travis WD, Brambilla E and Geisinger KR. Histological grading in lung cancer: one system for all or separate systems for each histological type? Eur Respir J 2016; 47: 720-723.
[5] Goodwin J, Neugent ML, Lee SY, Choe JH, Choi H, Jenkins DMR, Ruthenborg RJ, Robinson MW, Jeong JY, Wake M, Abe H, Takeda N, Endo H, Inoue M, Xuan Z, Yoo H, Chen M, Ahn JM, Minna JD, Helke KL, Singh PK, Shackelford DB and Kim JW. The distinct metabolic phenotype of lung squamous cell carcinoma defines selective vulnerability to glycolytic inhibition. Nat Commun 2017; 8: 15503.
[6] Land SR, Liu Q, Wickerham DL, Costantino JP and Ganz PA. Cigarette smoking, physical activity, and alcohol consumption as predictors of cancer incidence among women at high risk of breast cancer in the NSABP P-1 trial. Cancer Epidemiol Biomarkers Prev 2014; 23: 823-832.
[7] Drilon A, Rekhtman N, Ladanyi M and Paik P. Squamous-cell carcinomas of the lung: emerging biology, controversies, and the promise of targeted therapy. Lancet Oncol 2012; 13: e418-426.
[8] Haria D and Naora H. Homeobox gene deregulation: impact on the hallmarks of cancer. Cancer Hallm 2013; 1: 67-76.
[9] McGinnis W and Krumlauf R. Homeobox genes and axial patterning. Cell 1992; 68: 283-302.
[10] Platais C, Hakami F, Darda L, Lambert DW, Morgan R and Hunter KD. The role of HOX genes in head and neck squamous cell carcinoma. J Oral Pathol Med 2016; 45: 239-247.
[11] Shah N and Sukumar S. The Hox genes and their roles in oncogenesis. Nat Rev Cancer 2010; 10: 361-371.
[12] Christensen KL, Patrick AN, McCoy EL and Ford HL. The six family of homeobox genes in development and cancer. Adv Cancer Res 2008; 101: 93-126.
[13] Argiropoulos B and Humphries RK. Hox genes in hematopoiesis and leukemogenesis. Oncogene 2007; 26: 6766-6776.
[14] Morgan R, Boxall A, Harrington KJ, Simpson GR, Michael A and Pandha HS. Targeting HOX transcription factors in prostate cancer. BMC Urol 2014; 14: 17.
[15] Morgan R, Plowright L, Harrington KJ, Michael A and Pandha HS. Targeting HOX and PBX transcription factors in ovarian cancer. BMC Cancer 2010; 10: 89.
[16] Hayashida T, Takahashi F, Chiba N, Brachtel E, Takahashi M, Godin-Heymann N, Gross KW, Vivanco M, Wijendran V, Shioda T, Sgroi D, Donahoe PK and Maheswaran S. HOXB9, a gene overexpressed in breast cancer, promotes tumorigenicity and lung metastasis. Proc Natl Acad Sci U S A 2010; 107: 1100-1105.
[17] Shears L, Plowright L, Harrington K, Pandha HS and Morgan R. Disrupting the interaction between HOX and PBX causes necrotic and apoptotic cell death in the renal cancer lines CaKi-2 and 769-P. J Urol 2008; 180: 2196-2201.
[18] Morgan R, Simpson G, Gray S, Gillett C, Tabi Z, Spicer J, Harrington KJ and Pandha HS. HOX transcription factors are potential targets and markers in malignant mesothelioma. BMC Cancer 2016; 16: 85.
[19] Mansour MA and Senga T. HOXD8 exerts a tumor-suppressing role in colorectal cancer as an apoptotic inducer. Int J Biochem Cell Biol 2017; 88: 1-13.
[20] Bhatlekar S, Fields JZ and Boman BM. HOX genes and their role in the development of human cancers. J Mol Med (Berl) 2014; 92: 811-823.
[21] Joo MK, Park JJ and Chun HJ. Impact of homeobox genes in gastrointestinal cancer. World J Gastroenterol 2016; 22: 8247-8256.
[22] He YX, Song XH, Zhao ZY and Zhao H. HOXA13 upregulation in gastric cancer is associated with enhanced cancer cell invasion and epithelial-to-mesenchymal transition. Eur Rev Med Pharmacol Sci 2017; 21: 258-265.
[23] Qu LP, Zhong YM, Zheng Z and Zhao RX. CDH17 is a downstream effector of HOXA13 in modulating the Wnt/beta-catenin signaling pathway in gastric cancer. Eur Rev Med Pharmacol Sci 2017; 21: 1234-1241.
[24] Zhang SR, Yang JK, Xie JK and Zhao LC. Long noncoding RNA HOTTIP contributes to the progression of prostate cancer by regulating HOXA13. Cell Mol Biol (Noisy-le-grand) 2016; 62: 84-88.
[25] Duan R, Han L, Wang Q, Wei J, Chen L, Zhang J, Kang C and Wang L. HOXA13 is a potential GBM diagnostic marker and promotes glioma invasion by activating the Wnt and TGF-beta pathways. Oncotarget 2015; 6: 27778-27793.
[26] Sang Y, Zhou F, Wang D, Bi X, Liu X, Hao Z, Li Q and Zhang W. Up-regulation of long non-coding HOTTIP functions as an oncogene by regulating HOXA13 in non-small cell lung cancer. Am J Transl Res 2016; 8: 2022-2032.

[27] Kang JU. Characterization of amplification patterns and target genes on the short arm of chromosome 7 in early-stage lung adenocarcinoma. Mol Med Rep 2013; 8: 1373-1378.
[28] Rong M, He R, Dang Y and Chen G. Expression and clinicopathological significance of miR-146a in hepatocellular carcinoma tissues. Ups J Med Sci 2014; 119: 19-24.
[29] Chen G, Kronenberger P, Umelo IA, Teugels E and De Greve J. Quantification of epidermal growth factor receptor T790M mutant transcripts in lung cancer cells by real-time reverse transcriptase-quantitative polymerase chain reaction. Anal Biochem 2010; 398: 266-268.
[30] Huang da W, Sherman BT and Lempicki RA. Systematic and integrative analysis of large gene lists using DAVID bioinformatics resources. Nat Protoc 2009; 4: 44-57.
[31] Huang da W, Sherman BT and Lempicki RA. Bioinformatics enrichment tools: paths toward the comprehensive functional analysis of large gene lists. Nucleic Acids Res 2009; 37: 1-13.
[32] Hou J, Aerts J, den Hamer B, van Ijcken W, den Bakker M, Riegman P, van der Leest C, van der Spek P, Foekens JA, Hoogsteden HC, Grosveld F and Philipsen S. Gene expression-based classification of non-small cell lung carcinomas and survival prediction. PLoS One 2010; 5: e10312.
[33] Garber ME, Troyanskaya OG, Schluens K, Petersen S, Thaesler Z, Pacyna-Gengelbach M, van de Rijn M, Rosen GD, Perou CM, Whyte RI, Altman RB, Brown PO, Botstein D and Petersen I. Diversity of gene expression in adenocarcinoma of the lung. Proc Natl Acad Sci U S A 2001; 98: 13784-13789.
[34] Abate-Shen C. Deregulated homeobox gene expression in cancer: cause or consequence? Nat Rev Cancer 2002; 2: 777-785.
[35] Feng J, Yang H, Zhang Y, Wei H, Zhu Z, Zhu B, Yang M, Cao W, Wang L and Wu Z. Tumor cell-derived lactate induces TAZ-dependent upregulation of PD-L1 through GPR81 in human lung cancer cells. Oncogene 2017; [Epub ahead of print].
[36] Giatromanolaki A, Sivridis E, Arelaki S and Koukourakis MI. Expression of enzymes related to glucose metabolism in non-small cell lung cancer and prognosis. Exp Lung Res 2017; 1-8.
[37] Zhang B, Zheng A, Hydbring P, Ambroise G, Ouchida AT, Goiny M, Vakifahmetoglu-Norberg H and Norberg E. PHGDH defines a metabolic subtype in lung adenocarcinomas with poor prognosis. Cell Rep 2017; 19: 2289-2303.
[38] Berridge MJ. The inositol trisphosphate/calcium signaling pathway in health and disease. Physiol Rev 2016; 96: 1261-1296.
[39] Wang Y, He J, Zhang S and Yang Q. Intracellular calcium promotes radioresistance of non-small cell lung cancer A549 cells through activating Akt signaling. Tumour Biol 2017; 39: 1010428317695970.
[40] Guo X, Zhu X, Zhao L, Li X, Cheng D and Feng K. Tumor-associated calcium signal transducer 2 regulates neovascularization of non-small-cell lung cancer via activating ERK1/2 signaling pathway. Tumour Biol 2017; 39: 1010428317694324.
[41] Wang T, Liang Y, Thakur A, Zhang S, Liu F, Khan H, Shi P, Wang N, Chen M and Ren H. Expression and clinicopathological significance of S100 calcium binding protein A2 in lung cancer patients of Chinese Han ethnicity. Clin Chim Acta 2017; 464: 118-122.
[42] Kim EJ and Juhnn YS. Cyclic AMP signaling reduces sirtuin 6 expression in non-small cell lung cancer cells by promoting ubiquitin-proteasomal degradation via inhibition of the Raf-MEK-ERK (Raf/mitogen-activated extracellular signal-regulated kinase/extracellular signal-regulated kinase) pathway. J Biol Chem 2015; 290: 9604-9613.
[43] Allam M, Bertrand R, Zhang-Sun G, Pappas J and Viallet J. Cholera toxin triggers apoptosis in human lung cancer cell lines. Cancer Res 1997; 57: 2615-2618.
[44] Choi YJ, Oh JM, Kim SY, Seo M and Juhnn YS. Stimulatory heterotrimeric GTP-binding protein augments cisplatin-induced apoptosis by up-regulating Bak expression in human lung cancer cells. Cancer Sci 2009; 100: 1069-1074.
[45] Shibata K, Tanaka S, Shiraishi T, Kitano S and Mori M. G-protein gamma 7 is down-regulated in cancers and associated with p 27kip1-induced growth arrest. Cancer Res 1999; 59: 1096-1101.
[46] Shibata K, Mori M, Tanaka S, Kitano S and Akiyoshi T. Identification and cloning of human G-protein gamma 7, down-regulated in pancreatic cancer. Biochem Biophys Res Commun 1998; 246: 205-209.
[47] Ohta M, Mimori K, Fukuyoshi Y, Kita Y, Motoyama K, Yamashita K, Ishii H, Inoue H and Mori M. Clinical significance of the reduced expression of G protein gamma 7 (GNG7) in oesophageal cancer. Br J Cancer 2008; 98: 410-417.
[48] Davis CA 3rd, Pearce WH, Haines GK, Shah M and Koch AE. Increased ICAM-1 expression in aortic disease. J Vasc Surg 1993; 18: 875-880.
[49] Yang L, Lee MM, Leung MM and Wong YH. Regulator of G protein signaling 20 enhances cancer cell aggregation, migration, invasion and adhesion. Cell Signal 2016; 28: 1663-1672.

[50] Song Y, Li A, Zhang L and Duan L. Expression of G protein-coupled receptor 56 is associated with tumor progression in non-small-cell lung carcinoma patients. Onco Targets Ther 2016; 9: 4105-4112.
[51] Yang Z, Zhuan B, Yan Y, Jiang S and Wang T. Identification of gene markers in the development of smoking-induced lung cancer. Gene 2016; 576: 451-457.
[52] Gusenbauer S, Zanucco E, Knyazev P and Ullrich A. Erk2 but not Erk1 regulates crosstalk between Met and EGFR in squamous cell carcinoma cell lines. Mol Cancer 2015; 14: 54.
[53] Li J, Wang J, Chen Y, Yang L and Chen S. A prognostic 4-gene expression signature for squamous cell lung carcinoma. J Cell Physiol 2017; 232: 3702-3713.
[54] Kang JH, Mori T, Kitazaki H, Niidome T, Takayama K, Nakanishi Y and Katayama Y. Serum protein kinase Calpha as a diagnostic biomarker of cancers. Cancer Biomark 2013; 13: 99-103.
[55] Kang JH, Mori T, Kitazaki H, Niidome T, Takayama K, Nakanishi Y and Katayama Y. Kinase activity of protein kinase calpha in serum as a diagnostic biomarker of human lung cancer. Anticancer Res 2013; 33: 485-488.
[56] Vaskovicova K, Szabadosova E, Cermak V, Gandalovicova A, Kasalova L, Rosel D and Brabek J. PKCalpha promotes the mesenchymal to amoeboid transition and increases cancer cell invasiveness. BMC Cancer 2015; 15: 326.
[57] Abera MB and Kazanietz MG. Protein kinase Calpha mediates erlotinib resistance in lung cancer cells. Mol Pharmacol 2015; 87: 832-841.